

Verification of a dynamical scaling for the pair correlation function during the slow drainage of a porous medium

M. Moura^{*1}, K. J. Måløy¹, E. G. Flekkøy¹, and R. Toussaint²

¹*Department of Physics, University of Oslo - PO Box 1048, Blindern, N-0316, Oslo, Norway.*

²*Université de Strasbourg, CNRS, IPGS UMR 7516 - 5 rue René Descartes, 67084, Strasbourg, France.*

April 17, 2019

We give experimental grounding for the remarkable observation made by Furuberg et al. in Ref. [1] of an unusual dynamic scaling for the pair correlation function $N(r, t)$ during the slow drainage of a porous medium. The authors of that paper have used an invasion percolation algorithm to show numerically that the probability of invasion of a pore at a distance r away and after a time t from the invasion of another pore, scales as $N(r, t) \propto r^{-1} f(r^D/t)$, where D is the fractal dimension of the invading cluster and the function $f(u) \propto u^{1.4}$, for $u \ll 1$ and $f(u) \propto u^{-0.6}$, for $u \gg 1$. Our experimental setup allows us to have full access to the spatiotemporal evolution of the invasion, which was used to directly verify this scaling. Additionally, we have connected two theoretical results from the literature to explain the functional dependency of $N(r, t)$ and the scaling exponent for the short-time regime ($t \ll r^D$). A new theoretical argument was developed to explain the long-time regime exponent ($t \gg r^D$).

The slow drainage of a porous medium is characterized by a rich intermittent dynamics of invasion bursts, typically occurring at several time and length scales [2–4]. Similar intermittent activity is observed in a wide variety of physical, biological and social systems [5–17]. The ubiquity of intermittent phenomena is an indication that its origin is not expected to depend on specific system-dependent details. It is generally associated to the competition between an adaptive external driving force and an internal random resistance against that force [3, 18]. Energy is slowly injected by the external force during stable periods which are abruptly interrupted by sudden dissipative events occurring at a much faster time scale [19–21]. In the case of two-phase flows in porous media, the external force could come from a syringe pump or an applied pressure difference across the sample, while the internal resistance is caused by the pore-throats in the sample that are invaded during the flow [2–4].

The balance between viscous, capillary and gravitational forces [22–25] generates several interesting invasion patterns in porous media flows, ranging from compact invasion [26–28] to fractal structures [29–32]. Although the pattern morphology has been well studied, very few studies have focused on its dynamical features [3, 4, 18, 33, 34], due in part to the difficulty of simultaneously analyzing detailed invasion data in both time and space domains. Single pore invasion events in rocks have only recently been imaged in real-time via mod-

ern X-ray microtomography techniques [33, 35], but extending those techniques to study pattern formations in rocks at the larger scales, while keeping single-pore resolution, remains a challenge.

The experimental constraints fueled the development of several numerical algorithms. Invasion percolation (IP) [36, 37], diffusion-limited aggregation (DLA) [29, 38, 39] and anti-DLA [39] have been employed in the simulation of, respectively, slow drainage (capillary fingering), fast drainage (viscous fingering) and stable imbibition (compact growth) [40]. Using an IP model, Furuberg et al. [1] have addressed the following question: given that a reference pore located at position \mathbf{r}_0 is invaded at a time t_0 , what is the probability that a second pore located at position \mathbf{r}_1 is invaded at some later time t_1 ? After the vanishing of transitional effects, the probability should only be a function of the relative quantities $r = |\mathbf{r}_1 - \mathbf{r}_0|$ and $t = t_1 - t_0$. The authors have defined a pair correlation function $N(r, t)$, such that $N(r, t)drdt$ gives the answer to the question, i.e., it is the probability of invasion of a pore located between distances r and $r + dr$ and at a time between t and $t + dt$ with respect to the invasion of the reference pore. By considering theoretical arguments related to the normalization of $N(r, t)$ and the connection between $N(r, t)$ and the pair connectedness function, the authors have suggested the form

$$N(r, t) = r^{-1} f\left(\frac{r^D}{t}\right), \quad (1)$$

^{*}Corresponding author (marcel.moura@fys.uio.no)

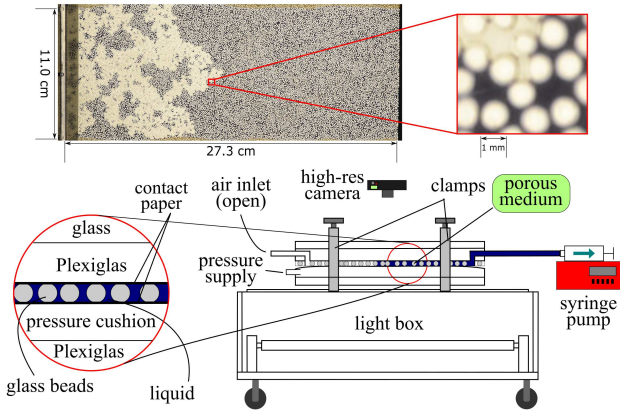


Figure 1: Diagram of the experimental setup. On top we show an image of the flow and in the detail a zoom in section of the porous network, the defending wetting phase (liquid, blue) and the invading non-wetting phase (air, white).

where the dynamical exponent D corresponds to the fractal dimension of the invaded front [41,42]. The IP simulations employed in that study confirmed the validity of Eq. (1) numerically and found out additionally that the function $f(u)$ presents the unusual scaling

$$f(u) \propto \begin{cases} u^{1.4} & \text{if } u \ll 1 \\ u^{-0.6} & \text{if } u \gg 1 \end{cases} \quad (2)$$

In the current work, we have demonstrated these results experimentally, almost 30 years after the original findings of Furuberg et al. [1].

Fig. 1 shows a diagram of the experimental setup. A quasi-2D porous network formed by a monolayer of glass beads, with diameters a in the range $1.0\text{mm} < a < 1.2\text{mm}$, is placed inside the gap of a modified Hele-Shaw cell. The beads are kept in place by a pressurized cushion placed on the bottom plate of the cell. The porous medium is initially saturated with a viscous liquid (wetting phase), composed of glycerol (80% in weight) and water (20% in weight), having kinematic viscosity $\nu = 4.25 \cdot 10^{-5} \text{m}^2/\text{s}$, density $\rho = 1.205 \text{g/cm}^3$ and surface tension $\gamma = 0.064 \text{N.m}^{-1}$ (see Ref. [43] for additional details). The outlet channel is connected to a syringe pump, from which liquid can be slowly withdrawn at a constant rate of $\approx 0.0050 \text{ml/min} \approx 0.14 \text{pore/s}$, thus assuring that the dynamics happens in the capillary regime, in which capillary forces dominate over viscous ones [32]. Air (non-wetting phase) enters from a width-spanning inlet channel, which is kept open to the atmosphere. Once the capillary pressure (difference in pressure between the non-wetting and wetting phases) is large enough to overcome the threshold associated with a given pore-throat, the invasion of one or more pores happens,

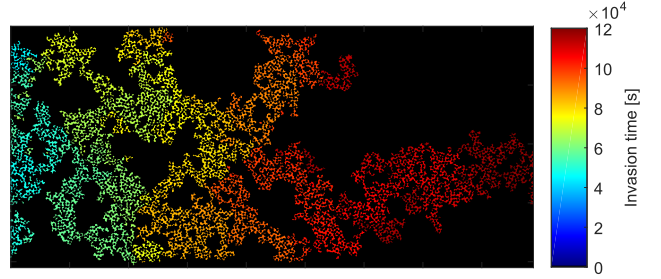


Figure 2: Spatiotemporal map of the invasion up to breakthrough (the average flow direction is from left to right). The colormap shows the elapsed time for the invasion of a given pore (in seconds). The experiment lasts $\approx 33h$.

and viscous pressure drops are triggered within the medium, thus dissipating energy [3,44]. Pictures are taken every 34s which leads to an average number of $K \approx 4.7$ invaded pores per image (average pore invasion time of $t_p = 7.2\text{s}$). The capillary number, $Ca = \rho\nu v/\gamma$, where v is a characteristic velocity (the ratio between a characteristic pore length and its time of invasion), is computed to be $Ca = 1.1 \cdot 10^{-4}$. The choice of a slow constant withdrawal rate reflects the fact that in the IP algorithm employed in Ref. [1], viscous drops are neglected and exactly 1 pore (numerical site) is invaded per time step.

Fig. 2 shows the spatiotemporal map of the invasion. The experiment stops at breakthrough, i.e., when the air phase first percolates through the model. Only the central 90% of the model's length (inlet-outlet direction) is considered, in order to avoid possible boundary effects [43]. The information content in this map is similar to that in the IP simulations, namely the position and invasion times of all pores, thus allowing the computation of the pair correlation function $N(r, t)$. In order to precisely locate the position of all pores in the sample, we performed a Delaunay triangulation [45] of the points marking the centers of all glass beads and then identified the centroid of each Delaunay triangle as a pore center. In the IP simulations [1], the time t is naturally measured as the number of invaded pores, whereas in our experiments we measure the time in terms of the image number t_I . The conversion between t_I and t is given by $t_I = t/K$, where K is the average number of pores invaded per image.

For a given reference pore, one can produce a histogram of the euclidean distances r of all pores invaded between times t_I and $t_I + \Delta t_I$ after the invasion of that reference pore. By seeing each invaded pore in the system as a reference for the production of one such histogram and then adding them up, we obtain the function $N(r, t)$ (apart from a normalization constant). We have chosen $\Delta t_I = 2$ images such as to guarantee that a small number of pore invasion events

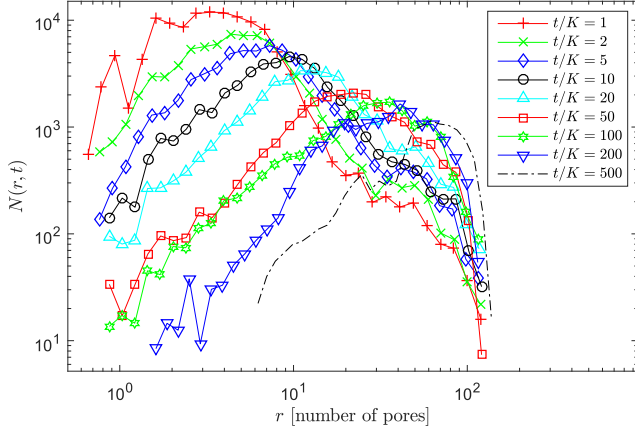


Figure 3: Pair correlation function $N(r, t)$ as a function of the distance r for 9 times t (shown in the figure).

(given, on average, by $\Delta t_I K \approx 9.4$) would be present on each histogram. We have tested different values of Δt_I in the range $1 \leq \Delta t_I \leq 5$ and the results presented did not change significantly, since the experiment duration ($\approx 33h$) is much longer than the time between images ($\approx 34s$).

The measured function $N(r, t)$ is shown in Fig. 3 for 9 fixed values of time $t/K = t_I$ (shown in the legend). The distance r is measured in pore length units (euclidean distance divided by a characteristic interpore distance $r_p = 0.92mm$). $N(r, t)$ presents a peak indicating a maximum probability of invasion at a certain relative distance r_t which increases with time (since the air-liquid interface had more time to move, pores farther away can be invaded). The validity of Eq. (1) is proved by using this equation to collapse the data from Fig. 3. The result, shown in Fig. 4, indicates that the product $N(r, t)r$ is indeed a function only of the reduced variable $u = r^D/t$ and not of r and t separately (the fractal dimension of the invasion cluster was measured to be $D = 1.75$). This confirms the validity of the dynamic scaling in Eq. (1). The fact that the product $N(r, t)r$ is peaked around $r^D/t = 1$ (with r and t measured in terms of pore length and average pore invasion time units) indicates that the most probable place for invasion occurs at a distance $r = t^{1/D}$, as noted in [1]. If one chooses another set of measuring units, the maximum changes to r_p^D/t_p , where r_p and t_p are the typical interpore distance and pore invasion time in the new units. We also show in Fig. 4 guide-to-eye lines with the scaling for the function $f(u)$, from Eq. (2). We see that both scaling regimes $u^{1.4}$ for $u \ll 1$ and $u^{-0.6}$ for $u \gg 1$ are well reproduced by the experiments (solid thick lines). Indeed, even the deviation from the scaling observed as the dropping curves for large times and $u \gg 1$ (related to finite-size effects) are also in agreement with the simulations presented in [1].

Next we provide a theoretical analysis to explain the

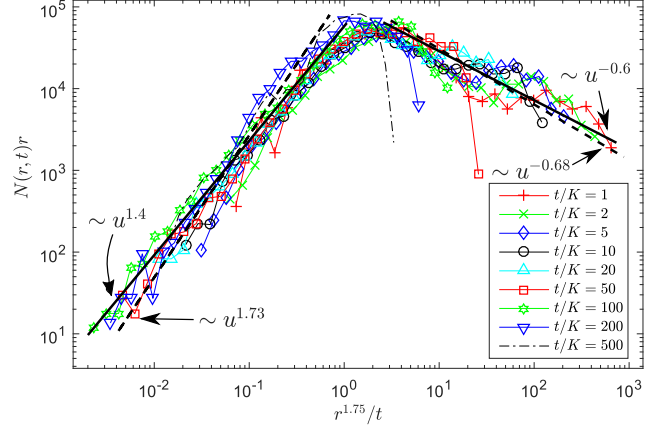


Figure 4: Data collapsing for the product $N(r, t)r$ as a function of the reduced variable $u = r^D/t$ for 9 different fixed times (see legend). We also show the scaling regimes for $u \ll 1$ and $u \gg 1$ from Eq. (2), as reported by Furuberg et al. [1] (thick solid lines) and the respective theoretical predictions (thick dashed lines).

origin of this scaling behavior. We begin by linking two important contributions to the literature on this topic, the works by Roux and Guyon [46] and Maslov [47]. Roux and Guyon [46] have analyzed the distribution of temporal avalanches in the time series of threshold values from an IP model and proposed an analytical prediction for the unusual scaling presented in Eqs. (1) and (2). Later on, Maslov [47] pointed out some inconsistencies in the assumptions used by Roux and Guyon [46], which interfered with their estimation for the exponents in Eq. (2). Nevertheless, their reasoning to justify the functional form behind Eqs. (1) and (2) still applies. By taking into account the results of Ref. [47], into the analysis performed in Ref. [46], we obtain a consistent value for the short-time exponent in Eq. (2) (for $u \gg 1$ or $t \ll r^D$). The analysis for the long-time exponent (for $u \ll 1$ or $t \gg r^D$) will require some additional considerations, as shown later.

Following Ref. [46], for a given time interval t , the distribution of backwards temporal avalanches Θ (as defined in [46] and also in [47]) that are larger than t is assumed to follow the power law

$$P_t(\Theta) \propto \frac{1}{t} \left(\frac{\Theta}{t} \right)^{-\tau_b^{all}} H(\Theta - t), \quad (3)$$

where $H(x) = 1$ for $x > 0$ and $H(x) = 0$ otherwise. The dependency on t in the prefactor follows from the normalization in the interval $t < \Theta < \infty$ [46]. We remind that in the IP model, the time corresponds to the size (mass) of the invaded cluster, measured in number of pores. For a cluster of size Θ , the distribution $Q_\Theta(r)$ of distances r between pores in that cluster is also as-

sumed to follow a power law,

$$Q_\Theta(r) \propto \Theta^{-(1+\alpha)/D} r^\alpha H\left(\Theta^{1/D} - r\right), \quad (4)$$

for r in the interval $0 < r < \Theta^{1/D}$, where again the dependency on Θ in the prefactor is obtained by the normalization in the interval $0 < r < \Theta^{1/D}$ [46]. The pair correlation function $N(r, t)$ is then given by

$$N(r, t) = \int_0^\infty P_t(\Theta) Q_\Theta(r) d\Theta, \quad (5)$$

which, using Eqs. (3) and (4) leads to

$$N(r, t)r = f\left(\frac{r^D}{t}\right) = \begin{cases} \left(\frac{r^D}{t}\right)^{\frac{1+\alpha}{D}} & \text{if } \frac{r^D}{t} \ll 1 \\ \left(\frac{r^D}{t}\right)^{1-\tau_b^{all}} & \text{if } \frac{r^D}{t} \gg 1 \end{cases}. \quad (6)$$

The insightful argumentation provided by Roux and Guyon [46] naturally generates the correct functional form of Eqs. (1) and (2). Nevertheless their subsequent analysis for the numerical values of the exponents presents some inconsistent assumptions, as noted by Maslov [47]. The exponent τ_b^{all} characterizing the distribution of all backwards avalanches was shown [47] to be given by $\tau_b^{all} = 3 - \tau$, where $\tau = 1 + (D_e - 1/\nu)/D$ is the cluster size distribution exponent (first derived in [48], and verified experimentally in [49]), D and D_e are respectively the fractal dimensions of the growing cluster and its boundary and $\nu = 4/3$ is the exponent characterizing the divergence of the correlation length [37, 42]. Using the values $D = 1.82$ and $D_e = 4/3$ (external perimeter growth) [37, 42], we find that the short-time exponent is

$$1 - \tau_b^{all} = -1 + \left(\frac{D_e - 1/\nu}{D}\right) \implies 1 - \tau_b^{all} = -0.68, \quad (7)$$

which is consistent with our measurements and very close to the value -0.6 reported in Ref. [1], see Fig. 4.

The computation of the long-time exponent brings additional challenges related to the difficulty in correctly estimating the exponent α in Eq. (4), as pointed out by Roux and Guyon [46]. With that in mind, we take an alternative approach here. Consider the situation in which a pore-throat that gives access to a pore at position \mathbf{r}_1 has been reached by the liquid air interface at a time t_* . From that moment on, that pore-throat and the accompanying pore-body at \mathbf{r}_1 are available to the invasion. Let us focus here on the case in which this particular pore-throat has a relatively high value of capillary pressure threshold, meaning that its invasion will typically take a long time to occur. This type of invasion event lies in the long-time regime, for which $t \gg r^D$, and we are interested in addressing their relative probability of occurrence.

For the invasion of the pore at \mathbf{r}_1 to happen exactly at time $t = t_1$, a set of two well defined conditions must be verified: 1) the capillary pressure at time $t = t_1$ must reach a historically high value since time $t = t_*$ and 2) the pore-throat at \mathbf{r}_1 must have the lowest value of capillary pressure threshold among those that belong to the liquid air interface at time $t = t_1$ (i.e., it is the widest pore-throat available at the moment). Let us initially address condition 1). Consider the capillary pressure signal as the discrete time series formed by the sequence of the capillary pressure thresholds $p(t)$ associated with the invasion of successive pore-throats. If the system is in a statistical steady state (say, the flow has been going for a long time and happens in a long rectangular cell of large but finite width), the capillary pressure signal fluctuates around some well defined average and the historical maximum is equally likely to occur anywhere in the interval $t_* < t \leq t_1$. The probability that it occurs at the extreme point $t = t_1$ is then proportional to $1/(t_1 - t_*)$. Once the capillary pressure reaches the historical maximum at $t = t_1$, the invasion at \mathbf{r}_1 can happen. Next, we consider condition 2) and calculate the probability that the particular pore-throat in question is the one with the lowest threshold. Since the capillary pressure at time $t = t_1$ has reached a historical maximum, it is the first time that the pore-throats on the interface have been tested against such a high value of capillary pressure, and at this pressure they all have the same invasion probability. The number of sites N_I that belong to the interface of the cluster that has grown since time $t = t_0$ (when the reference pore at \mathbf{r}_0 was invaded) scales as $N_I \propto t^{D_e/D}$. The probability that the particular pore-throat at \mathbf{r}_1 is the widest is simply given by $1/N_I$. (We have made the assumption that the invasion of the pore at \mathbf{r}_1 does not depend on invasion events that happened earlier than the invasion at \mathbf{r}_0 . In the limit $t = t_1 - t_0 \rightarrow \infty$, this approximation becomes exact). By considering the probability of simultaneously satisfying conditions 1) and 2), we have

$$N(r, t) \propto \frac{1}{(t_1 - t_*)} \frac{1}{t^{D_e/D}} \approx \frac{1}{t^\xi}, \quad (8)$$

where $\xi = 1 + D_e/D$ and we used the fact that in the limit of large times, $t_1 - t_* \approx t_1 - t_0 = t$. The r dependence in the previous equation can be obtained by considering again Eq. (1). Since the product $N(r, t)r$ is a function only of the reduced variable r^D/t , we have that in the long-time regime,

$$N(r, t) \propto \frac{1}{r} \left(\frac{r^D}{t}\right)^\xi. \quad (9)$$

Using the literature values $D = 1.82$ and $D_e = 4/3$ [37, 42], we find $\xi = 1.73$. This value is higher than the exponent $\xi = 1.4$ reported by Furuberg et al. [1], but is

consistent with the experimental data, particularly in the region on the extreme left of Fig. 4, where $t \gg r^D$ and the approximations of the model should hold best.

After the aged (hard) site at \mathbf{r}_1 is invaded, we could in principle have the invasion of easier pores in its vicinity that would also contribute to the counting in the long-time regime of $N(r, t)$. Although the argument made here counts explicitly only the aged (hard) sites, the invasion of easier ones in the long-time regime is conditioned to the prior invasion of an aged site and therefore should not change the temporal scaling of Eq. (8).

In the present paper we have given experimental validation to the unusual dynamic scaling for the pair correlation function $N(r, t)$ during the slow drainage of a porous medium, first observed by Furuberg et al. [1] nearly 30 years ago. Although this important result has been reproduced in other numerical works [50], to the best of our knowledge, the experimental verification presented here is new. The functional dependency of Eqs. (1) and (2) was first obtained by Roux and Guyon [46]. Nevertheless, as pointed out by Maslov [47], some inconsistencies in the assumptions made in that work were reflected in the suggested values for the exponents in Eq. (2). By incorporating the corrections outlined by Maslov into the work of Roux and Guyon, we found out that both approaches lead to the same predictions for the short-time exponent, which agrees well with our measurements. A new theoretical explanation for the long-time exponent has also been provided.

We gratefully acknowledge the support from the University of Oslo, University of Strasbourg, the Norwegian Research Council through the FRINAT Grant No. 205486, the CNRS-INSU ALEAS program and the EU Marie Curie ITN FLOWTRANS network.

References

- [1] L. Furuberg, J. Feder, A. Aharony, and T. Jøssang, “Dynamics of invasion percolation,” *Phys. Rev. Lett.*, vol. 61, pp. 2117–2120, 1988.
- [2] W. B. Haines, “Studies in the physical properties of soil. v. the hysteresis effect in capillary properties, and the modes of moisture distribution associated therewith,” *J. Agric. Sci.*, vol. 20, pp. 97–116, 1930.
- [3] K. J. Måløy, L. Furuberg, J. Feder, and T. Jøssang, “Dynamics of slow drainage in porous media,” *Phys. Rev. Lett.*, vol. 68, pp. 2161–2164, 1992.
- [4] L. Furuberg, K. J. Måløy, and J. Feder, “Intermittent behavior in slow drainage,” *Phys. Rev. E*, vol. 53, pp. 966–977, 1996.
- [5] L. F. Burlaga, “Intermittent turbulence in the solar wind,” *J. Geophys. Res.*, vol. 96, no. A4, pp. 5847–5851, 1991.
- [6] A. A. Ruzmaikin, J. Feynman, B. E. Goldstein, E. J. Smith, and A. Balogh, “Intermittent turbulence in solar wind from the south polar hole,” *J. Geophys. Res.*, vol. 100, no. A3, pp. 3395–3403, 1995.
- [7] K. Sneppen, P. Bak, H. Flyvbjerg, and M. H. Jensen, “Evolution as a self-organized critical phenomenon,” *Proc. Natl. Acad. Sci. U.S.A.*, vol. 92, no. 11, pp. 5209–5213, 1995.
- [8] M. A. F. Gomes, F. A. O. Souza, and V. P. Brito, “Persistence and intermittency in sliding of blocks,” *J. Phys. D: Appl. Phys.*, vol. 31, no. 22, p. 3223, 1998.
- [9] Y. Liu, P. Gopikrishnan, P. Cizeau, M. Meyer, C.-K. Peng, and H. E. Stanley, “Statistical properties of the volatility of price fluctuations,” *Phys. Rev. E*, vol. 60, pp. 1390–1400, 1999.
- [10] J. P. Sethna, K. A. Dahmen, and C. R. Myers, “Crackling noise,” *Nature*, vol. 410, no. 6825, pp. 242–250, 2001.
- [11] K. J. Måløy, S. Santucci, J. Schmittbuhl, and R. Toussaint, “Local waiting time fluctuations along a randomly pinned crack front,” *Phys. Rev. Lett.*, vol. 96, p. 045501, 2006.
- [12] M. Grob, J. Schmittbuhl, R. Toussaint, L. Rivera, S. Santucci, and K. J. Måløy, “Quake catalogs from an optical monitoring of an interfacial crack propagation,” *Pure Appl. Geophys.*, vol. 166, no. 5, pp. 777–799, 2009.
- [13] R. Planet, S. Santucci, and J. Ortín, “Avalanches and non-gaussian fluctuations of the global velocity of imbibition fronts,” *Phys. Rev. Lett.*, vol. 102, p. 094502, 2009.
- [14] D. S. P. Salazar and G. L. Vasconcelos, “Stochastic dynamical model of intermittency in fully developed turbulence,” *Phys. Rev. E*, vol. 82, p. 047301, 2010.
- [15] S. Santucci, R. Planet, K. J. Måløy, and J. Ortín, “Avalanches of imbibition fronts: Towards critical pinning,” *EPL*, vol. 94, no. 4, p. 46005, 2011.
- [16] K. T. Tallakstad, R. Toussaint, S. Santucci, and K. J. Måløy, “Non-gaussian nature of fracture and the survival of fat-tail exponents,” *Phys. Rev. Lett.*, vol. 110, p. 145501, 2013.

- [17] M. Stojanova, S. Santucci, L. Vanel, and O. Ramos, “High frequency monitoring reveals aftershocks in subcritical crack growth,” *Phys. Rev. Lett.*, vol. 112, p. 115502, 2014.
- [18] F. Moebius and D. Or, “Interfacial jumps and pressure bursts during fluid displacement in interacting irregular capillaries,” *J. Colloid Interface Sci.*, vol. 377, no. 1, pp. 406 – 415, 2012.
- [19] Y. Pomeau and P. Manneville, “Intermittent transition to turbulence in dissipative dynamical systems,” *Commun. Math. Phys.*, vol. 74, no. 2, pp. 189–197, 1980.
- [20] Manneville, P., “Intermittency, self-similarity and $1/f$ spectrum in dissipative dynamical systems,” *J. Phys. France*, vol. 41, no. 11, pp. 1235–1243, 1980.
- [21] J. E. Hirsch, B. A. Huberman, and D. J. Scalapino, “Theory of intermittency,” *Phys. Rev. A*, vol. 25, pp. 519–532, 1982.
- [22] Y. Méheust, G. Løvoll, K. J. Måløy, and J. Schmittbuhl, “Interface scaling in a two-dimensional porous medium under combined viscous, gravity, and capillary effects,” *Phys. Rev. E*, vol. 66, p. 051603, 2002.
- [23] G. Løvoll, Y. Méheust, K. J. Måløy, E. Aker, and J. Schmittbuhl, “Competition of gravity, capillary and viscous forces during drainage in a two-dimensional porous medium, a pore scale study,” *Energy*, vol. 30, pp. 861–872, 2005.
- [24] D. Or, “Scaling of capillary, gravity and viscous forces affecting flow morphology in unsaturated porous media,” *Adv. Water Resour.*, vol. 31, no. 9, pp. 1129 – 1136, 2008.
- [25] S. Polak, Y. Cinar, T. Holt, and O. Torsæter, “An experimental investigation of the balance between capillary, viscous, and gravitational forces during CO₂ injection into saline aquifers,” *Energy Procedia*, vol. 4, pp. 4395–4402, 2011.
- [26] M. Cieplak and M. O. Robbins, “Influence of contact angle on quasistatic fluid invasion of porous media,” *Phys. Rev. B*, vol. 41, no. 16, pp. 11508–11521, 1990.
- [27] M. Trojer, M. L. Szulczewski, and R. Juanes, “Stabilizing fluid-fluid displacements in porous media through wettability alteration,” *Phys. Rev. Applied*, vol. 3, p. 054008, 2015.
- [28] R. Holtzman and E. Segre, “Wettability stabilizes fluid invasion into porous media via nonlocal, cooperative pore filling,” *Phys. Rev. Lett.*, vol. 115, p. 164501, 2015.
- [29] K. J. Måløy, J. Feder, and T. Jøssang, “Viscous fingering fractals in porous media,” *Phys. Rev. Lett.*, vol. 55, pp. 2688–2691, 1985.
- [30] R. Lenormand and C. Zarcone, “Invasion percolation in an etched network: Measurement of a fractal dimension,” *Phys. Rev. Lett.*, vol. 54, pp. 2226–2229, 1985.
- [31] R. Lenormand, “Flow through porous media: limits of fractal pattern,” *Proc. R. Soc. Lond. A*, vol. 423, no. 1864, pp. 159–16, 1989.
- [32] R. Lenormand and C. Zarcone, “Capillary fingering: Percolation and fractal dimension,” *Transport in Porous Media*, vol. 4, no. 6, pp. 599–612, 1989.
- [33] S. Berg *et al.*, “Real-time 3d imaging of Haines jumps in porous media flow,” *Proc. Natl. Acad. Sci. U.S.A.*, vol. 110, no. 10, pp. 3755–3759, 2013.
- [34] F. Moebius and D. Or, “Pore scale dynamics underlying the motion of drainage fronts in porous media,” *Water Resour. Res.*, vol. 50, no. 11, pp. 8441–8457, 2014.
- [35] T. Bultreys *et al.*, “Real-time visualization of Haines jumps in sandstone with laboratory-based microcomputed tomography,” *Water Resour. Res.*, vol. 51, no. 10, pp. 8668–8676, 2015.
- [36] D. Wilkinson and J. F. Willemsen, “Invasion percolation: a new form of percolation theory,” *J. Phys. A: Math. Gen.*, vol. 16, no. 14, pp. 3365–3376, 1983.
- [37] D. Stauffer, *Introduction to percolation theory*. London Bristol, PA: Taylor & Francis, 1994.
- [38] T. A. Witten and L. M. Sander, “Diffusion-limited aggregation, a kinetic critical phenomenon,” *Phys. Rev. Lett.*, vol. 47, pp. 1400–1403, 1981.
- [39] L. Paterson, “Diffusion-limited aggregation and two-fluid displacements in porous media,” *Phys. Rev. Lett.*, vol. 52, pp. 1621–1624, 1984.
- [40] R. Lenormand, E. Touboul, and C. Zarcone, “Numerical models and experiments on immiscible displacements in porous media,” *J. Fluid Mech.*, vol. 189, pp. 165–187, 1988.
- [41] B. Mandelbrot, *The fractal geometry of nature*. San Francisco: W.H. Freeman, 1982.
- [42] J. Feder, *Fractals*. New York: Plenum Press, 1988.
- [43] M. Moura, E.-A. Fiorentino, K. J. Måløy, G. Schäfer, and R. Toussaint, “Impact of sample geometry on the measurement of pressure-saturation curves: Experiments and simulations,”

Water Resour. Res., vol. 51, no. 11, pp. 8900–8926, 2015.

- [44] G. Løvøll, M. Jankov, K. Måløy, R. Toussaint, J. Schmittbuhl, G. Schäfer, and Y. Méheust, “Influence of viscous fingering on dynamic saturation-pressure curves in porous media,” *Transport in Porous Media*, vol. 86, no. 1, pp. 305–324, 2011.
- [45] D. Lee and B. Schachter, “Two algorithms for constructing a delaunay triangulation,” *Int. J. Comput. Inf. Sci.*, vol. 9, no. 3, pp. 219–242, 1980.
- [46] S. Roux and E. Guyon, “Temporal development of invasion percolation,” *J. Phys. A*, vol. 22, no. 17, p. 3693, 1989.
- [47] S. Maslov, “Time directed avalanches in invasion models,” *Phys. Rev. Lett.*, vol. 74, pp. 562–565, 1995.
- [48] N. Martys, M. O. Robbins, and M. Cieplak, “Scaling relations for interface motion through disordered media: Application to two-dimensional fluid invasion,” *Phys. Rev. B*, vol. 44, pp. 12294–12306, 1991.
- [49] M. Moura, K. J. Måløy, and R. Toussaint, “Critical behavior in porous media flow,” *eprint arXiv:1611.04210 [physics.flu-dyn]*, 2016.
- [50] M. Ferer, G. S. Bromhal, and D. H. Smith, “Spatial distribution of avalanches in invasion percolation: their role in fingering,” *Physica A*, vol. 311, no. 12, pp. 5 – 22, 2002.